Plant Biotechnology Journal (2007) **5**, pp. 615–626 doi: 10.1111/j.1467-7652.2007.00267.x

Efficiency of gene silencing in *Arabidopsis*: direct inverted repeats vs. transitive RNAi vectors

Sergei A. Filichkin[1], Stephen P. DiFazio[2], Amy M. Brunner[3], John M. Davis[4], Zamin K. Yang[5], Udaya C. Kalluri[5], Renee S. Arias[6], Elizabeth Etherington[6], Gerald A. Tuskan[5] and Steven H. Strauss[6]*

[1]*Department of Botany and Plant Pathology, Oregon State University, Corvallis, OR 97331, USA*
[2]*Department of Biology, West Virginia University, Morgantown, WV 26506-6057, USA*
[3]*Department of Forestry, Virginia Polytechnic Institute and State University, Blacksburg, USA*
[4]*School of Forest Resources and Conservation, Plant Molecular and Cellular Biology Program, University of Florida, Gainesville, FL 32611, USA*
[5]*Oak Ridge National Laboratory, P.O. Box 2008, Oak Ridge, TN 37831-6422, USA*
[6]*Department of Forest Science, Oregon State University, Corvallis, OR 97331, USA*

Received 31 January 2007;
revised 22 April 2007;
accepted 24 April 2007.
**Correspondence* (fax 541-737-1393;
e-mail steve.strauss@oregonstate.edu)

Summary

We investigated the efficiency of RNA interference (RNAi) in *Arabidopsis* using transitive and homologous inverted repeat (hIR) vectors. hIR constructs carry self-complementary intron-spliced fragments of the target gene whereas transitive vectors have the target sequence fragment adjacent to an intron-spliced, inverted repeat of heterologous origin. Both transitive and hIR constructs facilitated specific and heritable silencing in the three genes studied (*AP1*, *ETTIN* and *TTG1*). Both types of vectors produced a phenotypic series that phenocopied reduction of function mutants for the respective target gene. The hIR yielded up to fourfold higher proportions of events with strongly manifested reduction of function phenotypes compared to transitive RNAi. We further investigated the efficiency and potential off-target effects of *AP1* silencing by both types of vectors using genome-scale microarrays and quantitative RT-PCR. The depletion of *AP1* transcripts coincided with reduction of function phenotypic changes among both hIR and transitive lines and also showed similar expression patterns among differentially regulated genes. We did not detect significant silencing directed against homologous potential off-target genes when constructs were designed with minimal sequence similarity. Both hIR and transitive methods are useful tools in plant biotechnology and genomics. The choice of vector will depend on specific objectives such as cloning throughput, number of events and degree of suppression required.

Keywords: RNA interference, *Arabidopsis*, transitive gene silencing vectors.

Introduction

Post-transcriptional gene silencing (PTGS), also termed RNA interference (RNAi), is an effective tool for targeted modification of endogenous gene expression. RNAi has several advantages over conventional transgenic approaches. RNAi suppression is highly sequence-specific, yet it is possible to knock down multiple genes by targeting their conserved sequences. Reversible silencing can also be achieved by using inducible promoters (Chen *et al*., 2003; Lo *et al*., 2005).

While the basic processes underlying gene silencing are conserved across kingdoms, the specific RNAi mechanisms differ among species (reviewed by Baulcombe, 2004). The initiation of gene silencing is triggered by an inducer, typically a double-stranded RNA (dsRNA) homologous to the sequence of the target mRNA. Degradation of the target mRNA is associated with the production of small interfering RNAs (siRNAs) (reviewed by Baulcombe, 2004; Meister and Tuschl, 2004; Tomari and Zamore, 2005). PTGS of endogenes can also be triggered by endogenous *trans*-acting siRNAs (Vazquez *et al*., 2004) or microRNAs (Carrington and Ambros, 2003; Tang *et al*., 2003).

In plants and nematodes, efficient silencing requires an amplification step resulting in the production of secondary

siRNAs by *de novo* RNA synthesis implying activity of RNA-dependent RNA polymerase (RDR) (Sijen *et al*., 2001; Vaistij *et al*., 2002). In transgenic plants, RNAi targets are involved in the expansion of the pool of functional siRNAs, which can further serve as primers for the synthesis of dsRNA by RDR (Vaistij *et al*., 2002). This amplification step results in the production of siRNAs with identity not only to the dsRNA inducer sequence, but also to the adjacent regions of target mRNA. The phenomenon of silencing spreading along the mRNA sequence is termed transitive RNAi silencing (Sijen *et al*., 2001).

Transitive RNAi has been reported for nematodes (*Caenorhabditis elegans*) (Lipardi *et al*., 2001; Sijen *et al*., 2001), fungi (Nicolas *et al*., 2003) and plants (Hamilton *et al*., 1998; Voinnet *et al*., 1998; Wesley *et al*., 2001; Brummell *et al*., 2003). The direction of transitive silencing spreading along the target sequence depends on the organism. In the fungus *Mucor circinelloides*, transitive silencing travels in 5′→3′ direction (i.e. downstream relative to the inducer sequence) (Nicolas *et al*., 2003). In plants, transitive RNAi is bidirectional and can spread both in 5′→3′ (Braunstein *et al*., 2002) and 3′→5′ directions (Vaistij *et al*., 2002). The mechanism of transitive silencing in plants is poorly understood and its spreading and efficiency appear to be both sequence- and position-dependent. The efficiency of endogene suppression by transitive RNAi is also dependent on the length of sequence homology (Bleys *et al*., 2006). Transitive RNAi can also trigger off-target effects causing decrease in expression of the secondary genes without transcript homology to the inducing locus (Van Houdt *et al*., 2003).

Efficient silencing in plants can be achieved by using vectors with homologous inverted repeats (hIR) directly targeting a specific portion of the endogene (Waterhouse *et al*., 1998; Smith *et al*., 2000; Wesley *et al*., 2001; Helliwell and Waterhouse, 2005). Construction of such vectors can be laborious because of multiple cloning steps and potential instability of the intron-spliced inverted repeats (IR). Alternatively, RNAi could be triggered by a heterologous IR placed adjacent to the target sequence. Hamilton *et al*. (1998) reported that a presence of a short IR of the 5′-UTR of the tomato *ACC-oxidase* (*ACO1*) gene resulted in degradation of the endogenous *ACO1* and *ACO2* transcripts. Brummell *et al*. (2003) showed that systemic transitive silencing in tomato and *Arabidopsis* can be triggered by constructs containing a target endogene fragment 5′ of an IR of a 3′ untranslated region (UTR) of a heterologous sequence. Transitive RNAi vectors could be used for high throughput screening of cDNA libraries without any knowledge of the insert DNA sequence. Transitive vectors also have the advantage of generating stable constructs carrying target sequences of multiple unrelated genes.

Despite the widening application of RNA interference in plant functional genomics and biotechnology, to our knowledge no direct comparative study of the efficiency of transitive vs. hIR RNAi has been reported. Furthermore, transitive RNAi could potentially trigger off-target effects causing decreased expression of secondary genes without transcript homology to the inducing locus (Van Houdt *et al*., 2003), but the extent of this problem has not been adequately explored. To facilitate a direct comparison of the two approaches, we constructed GATEWAY™-based (Invitrogen, San Jose, CA, USA) plant binary vectors with similar backbones in which dsRNAs with homologous (direct) or heterologous (transitive) inverted repeats are driven by identical constitutive promoters. We tested the relative efficiency of hIR and transitive constructs targeting identical portions of several *Arabidopsis* genes. We further evaluated efficiency and potential off-target effects of *AP1* gene silencing by transitive and hIR constructs using genome-scale microarrays and quantitative PCR. We report broadly similar patterns of gene silencing and no evidence of significant off-target suppression caused by either RNAi method.

Results

Construction of vectors and cloning of RNAi target genes

For direct comparison of the efficiency of homologous IR and transitive RNAi silencing we constructed two binary vectors: pCAPD and pCAPT (Figure 1). The pCAPD vector is an RNAi vector designed for cloning of homologous self-complementary, intron-spliced inverted repeats of the target sequence. To facilitate rapid cloning, we introduced into pCAPD two GATEWAY cassettes (Invitrogen) in inverse orientation separated by the potato *PIV2* intron as described in the Experimental procedures. In the pCAPT vector, a single conversion cassette is located upstream of the inverted repeat of octopine synthase (*OCS*) terminator. In both pCAPD and pCAPT transcription of the short hairpin RNA (shRNA) is controlled by identical constitutive CaMV *35S* promoters and *OCS* terminators. A small 5′ fragment of green fluorescent protein (*GFP*) coding sequence was incorporated upstream of pCAPT recombination site. The *GFP* fragment allows monitoring transitive endogene silencing in plants constitutively expressing the *GFP* transgene (however, the efficiency of this approach has not been evaluated in our study).

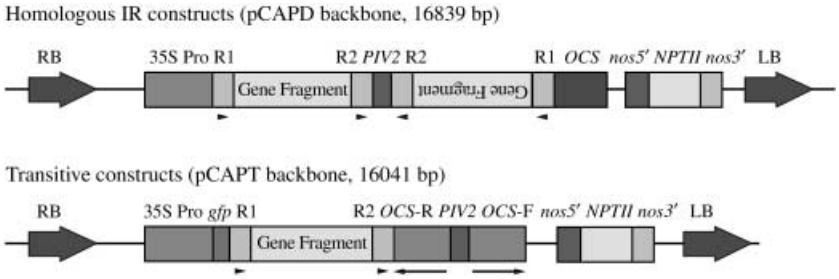

Figure 1 Schematic representation of vectors constructed for RNAi silencing using homologous (pCAPD) and heterologous (pCAPT) inverted repeat constructs. R1 and R2, *attR* recombination sites flanking a *ccdB* gene and a chloramphenicol-resistance gene (Cm^R) of GATEWAY vector conversion cassette, reading frame A (Invitrogen); 35S Pro: CaMV 35S promoter; *OCS*, octopine synthase terminator; *OCS*-F and *OCS*-R, *OCS* sequence fragments in forward (F) and reverse (R) orientations; *NPTII*, neomycin phosphotransferase II; *PIV2*, potato intron; LB and RB, left and right T-DNA borders, respectively; gfp, a fragment of *GFP*-coding sequence in pCAPT vector. Homologous IR and transitive RNAi constructs were made using pCAPD and pCAPT, respectively. Gene Fragment: location of *AP1*, *ETTIN*, or*TTG1* fragments. Vectors were constructed using a backbone of pART27 binary vector (Gleave, 1992) as described in the Experimental procedures. Arrowheads and arrows indicate orientations of *attR* recombination sites and *OCS* terminators, respectively. The map is not drawn to scale.

To evaluate the efficacy of PTGS caused by transitive and hIR RNAi constructs, we selected three *Arabidopsis* target genes with known expression patterns and well-characterized loss or reduction of function mutant phenotypes. This set included genes: (i) *APETALA1* (*AP1*) encoding a MADS domain transcription factor that specifies floral meristem identity (Mandel *et al*., 1992; Bowman *et al*., 1993); (ii) *ETTIN* (*ARF3*) encoding an auxin-responsive factor (Sessions and Zambryski, 1995); and (iii) *TRANSPARENT TESTA GLABRA1* (*TTG1*) encoding a WD40 repeat protein regulating trichome and root hair development (Walker *et al*., 1999). RNAi target fragments were designed with minimal sequence similarity to other homologous genes. Identical fragments of each gene were PCR amplified followed by GATEWAY cloning into hIR or transitive vectors (pCAPD or pCAPT, respectively) as described in the Experimental procedures. Resulting constructs were transformed into *Arabidopsis* and independent transgenic events were scored for loss-of-function phenotypes.

Efficiency of *AP1* gene silencing using transitive and hIR constructs

A total of 136 independent pCAPD-AP1 and pCAPT-AP1 primary kanamycin-resistant transformants were scored for frequencies of events showing *ap1* mutant-like reduction of function phenotype as described in the Experimental procedures. Both types of RNAi constructs generated multiple knockdown lines with a wide spectrum of morphological changes in floral organ development (Figure 2). Depending on the degree of floral morphology change all RNAi knockdown events were classified into three phenotypic series: P0, P1 and P2. Inflorescences of P0 plants were indistinguishable from the wild-type controls. Inflorescences of the P2 plants showed floral homeotic phenotype similar to that of *ap1-1* loss-of-function mutant (Bowman *et al*., 1993), including disruption of petal and sepal development. Enlarged sepals in P2 flowers were transformed into bract-like organs whereas petals were completely absent or rudimentary. P2 plants also frequently had a partial conversion of flowers into inflorescence shoots with secondary flowers developing in the axils of the first whorl organs of the primary flower. P2 inflorescences did not produce siliques and were completely sterile when grown at 15 °C. Floral organs of the P1 class displayed intermediate phenotypic features as compared to P0 and P2 with variable degrees of sterility among individual plants.

For both types of constructs the severity of the RNAi-induced *ap1* mutant-like phenotype was dependent on the growth temperature and on the flower position in the inflorescence shoot. Phenotypic changes in both pCAPD-AP1 and pCAPT-AP1 T1 transformants were manifested stronger when the plants were grown at lower temperature (15 °C). In contrast, plants grown at elevated temperatures (21–23 °C) showed weaker phenotypic changes (data not shown). Therefore, all phenotype scoring was done using plants grown at 15 °C. In P1 lines, the changes in flower morphology varied acropetally (i.e. were strongly enhanced at the bottom of the inflorescence shoot).

A total of 99 out of 136 primary transformants showed morphological abnormalities in floral organ development (Figure 2 and Supplementary Table S1). Fifty-four out of 65 pCAPD-AP1 and 45 out of 71 pCAPT-AP1 T_1 transgenic lines (83% hIR and 63% transitive RNAi, respectively) expressed *ap1* mutant-like phenotypes.

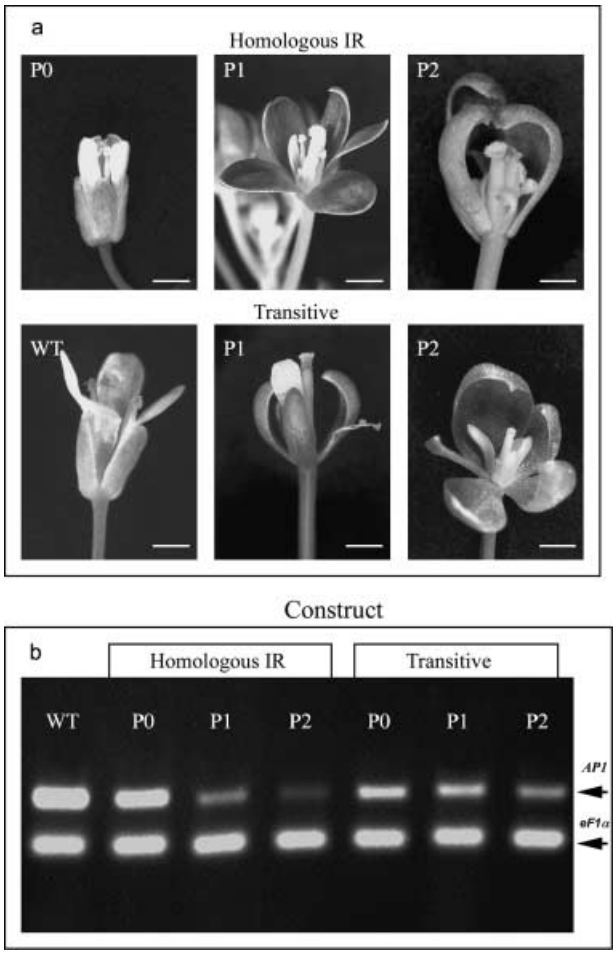

Figure 2 Silencing of *AP1* using transitive and homologous IR constructs. (a) The phenotypes associated with *AP1* gene silencing using transitive and hIR constructs. P0 phenotype was similar to the wild-type control. The flowers of P1 and P2 phenotypic classes developed leaf-like first whorl organs and leaf- or staminoid-like second whorl organs. The petals and stamens of P2 plants were reduced or absent and secondary flowers are frequently produced. The flowers in P2 did not develop siliques in plants grown at 15 °C. P1 comprised phenotypes intermediate between P0 and P2. Scale bars = 1.6, 2.0 and 2.5 mm (top row) and 2.0, 2.0 and 2.5 mm (bottom row), respectively. (b) Relative RT-PCR of *AP1* transcripts isolated from inflorescences of different phenotypic series. Each lane represents rRT-PCR products typically obtained for three independent events of the corresponding series. Arrows indicate positions of amplified fragments of the target (*AP1*) and internal control (elongation factor 1α, *eF1α*) transcripts.

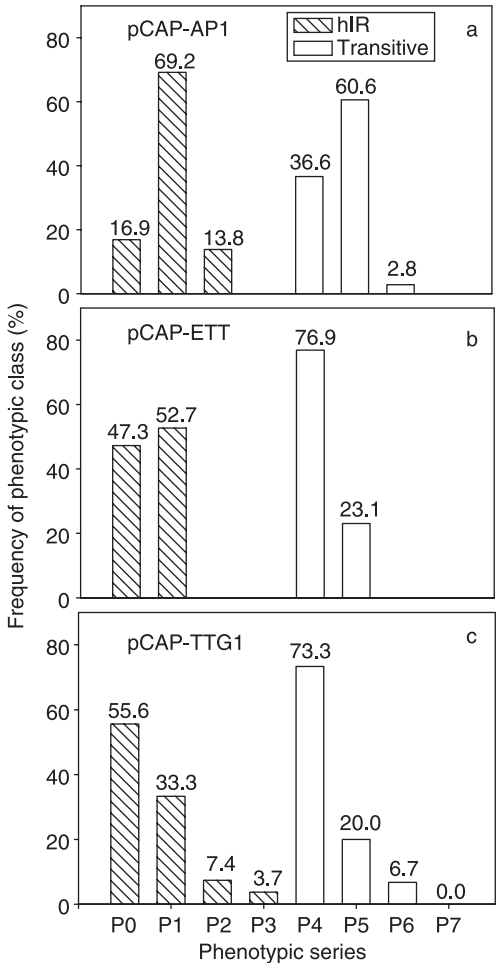

Figure 3 The frequencies of phenotypic series distribution among independent hIR and transitive RNAi transgenic lines. AP1 (pCAP-AP1) (a), ETTIN (pCAP-ETT) (b), and TTG1 (pCAP-TTG1) (c) knockdown lines of T_1 generation. hIR and transitive lines are shown by patterned and open bars, respectively. Numbers above the bars indicate the percentage of phenotypic class occurrence.

The majority of both transitive and hIR transgenics had an intermediate P1 phenotype (Figure 3). However, the proportion of events showing a strong P2 phenotype was fourfold lower among transitive than among hIR lines. Conversely, the weak P0 phenotype occurred with approximately twofold lower frequency among pCAPD-AP1 lines, suggesting that the hIR construct generated a higher proportion of the events with efficient suppression of *AP1* function. Statistical significance of phenotypic variation among individual events was evaluated using the χ^2-test for independence. We tested the null hypothesis that the distribution of P0, P1 and P2 phenotypic classes occurred with equal frequencies among hIR and transitive RNAi lines. This assumption was rejected ($\chi^2 = 10.3$, $P \leq 0.01$), suggesting that the shift towards weaker phenotypes observed among transitive lines was not due to chance alone.

To establish if the temperature sensitivity of *AP1* silencing phenotype is a feature of both transitive and hIR RNAi transgenics (as well as to obtain seeds from otherwise sterile flowers), the 5-week-old plants grown at 15 °C were incubated for 14 days at 23 °C. The pre-exiting inflorescences of all lines showing strong P2 phenotypes retained sterility at 23 °C as well. However, the newly grown inflorescences partially recovered the wild-type-like floral phenotype and

some produced siliques. This result suggested that the *AP1* silencing phenotype was equally temperature sensitive for both hIR and transitive RNAi and phenocopied enhancing effect of lower temperatures for several *ap1* mutant alleles (Bowman *et al*., 1993).

The phenotypic changes produced by both hIR and transitive RNAi constructs (including temperature dependency and acropetal distribution of the silencing phenotype) were stably inherited in T_2 and T_3 progeny and showed high (more than 90%) phenotype penetrance (Supplementary Table S1 and data not shown). Analysis of RNA synthesis using a semiquantitative relative RT-PCR method (rRT-PCR) indicated that *AP1* mRNA levels were depleted in P1 and P2 transgenics (Figure 2b). In contrast, P0 phenotypic series of both transitive and hIR transgenics had *AP1* RNA levels comparable to the wild-type plants.

Evaluation of the *AP1* gene silencing by hIR and transitive RNAi constructs using microarrays and quantitative RT-PCR

A total of 10 *Arabidopsis* whole-genome microarrays were hybridized with the RNA isolated from the inflorescences of wild-type controls, hIR and transitive RNAi lines as described in the Experimental procedures. Each construct was represented by two independent events showing the strong reduction of function phenotype P2. First, we identified microarray elements showing differential expression ($P < 0.05$) in at least one of the experiments. Then, we identified elements that were down- or up-regulated in hIR and/or transitive events at an arbitrarily chosen 1.5-fold difference level.

Hierarchical clustering of all microarray elements revealed three distinct groups corresponding to the (i) wild-type controls, (ii) hIR, and (iii) transitive RNAi events (Supplementary Figure S1). Both transitive and hIR RNAi events formed a joint-tree branch suggesting that both RNAi groups shared common features in gene expression patterns. Similar clustering of events according to the RNAi type was also evident for the group of 118 genes differentially expressed in both transitive and hIR transgenics (Figure 4). Differentially expressed genes showing similar expression patterns among experiments formed three major branches on the hierarchical tree. At least four major groups of genes were up- or down-regulated in both hIR and transitive RNAi transgenics as compared to the wild-type plants.

Several floral developmental genes in the *AP1* pathway showed that some of them were differentially expressed in at least one or both RNAi types of transgenics (Supplementary Figure S2). For example, *AP1, AP3*, *SEP2* and *SEP3* genes

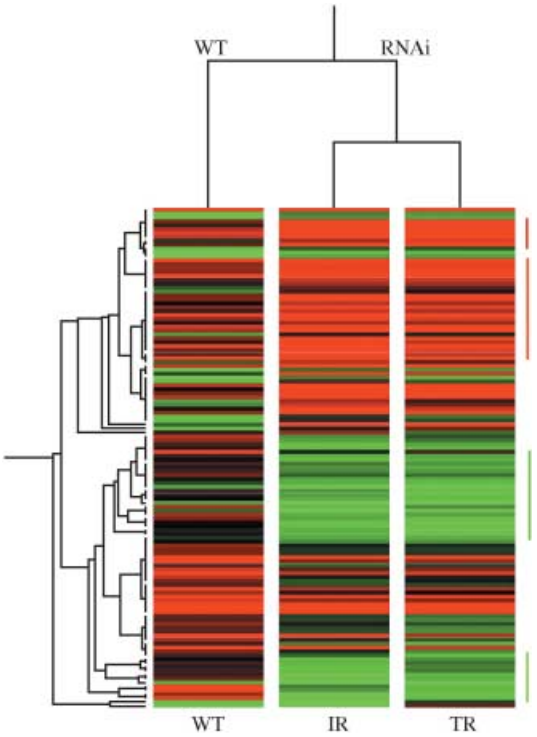

Figure 4 Hierarchical clustering of genes differentially regulated in inflorescences of both inverted repeat (IR) and transitive (TR) RNAi transgenics. Average signal intensities were first filtered for statistically significant differences (at $P < 0.05$ level) and then for change in expression at an arbitrarily chosen 1.5-fold level. Genes with similar or very low expression levels in all samples were filtered out. Classification of genes based on their expression pattern is displayed on the relationship tree to the left. The tree on top displays sample clustering according to common expression features among the genes. High and low levels of expression are shown by red and green colours, respectively. Major up- and down-regulated clusters of genes are indicated on right by red and green vertical lines, respectively. Hierarchical analysis was performed using GeneSpring GX 7.2 software (Agilent Technologies).

were down-regulated in both hIR and transitive lines. In contrast, *CAL* and *PI* were down-regulated ($P \leq 0.05$) in hIR but not in transitive lines. The expression of several housekeeping genes such as *EF1α* did not show significant variation among tested lines, suggesting that the differential expression of the above floral genes is likely to be associated with *AP1* silencing.

To validate microarray results we further investigated expression of *AP1* and three other floral developmental genes in the *AP1* regulatory pathway by quantitative reverse transcription PCR (qRT-PCR). The levels of *AP1* mRNA were depleted in inflorescences of independent pCAPD-AP1 and pCAPT-AP1 events showing a strong P2 phenotype (Figure 5a). In contrast, the absence of a visible phenotype in P0 transformants coincided with the accumulation of *AP1* RNA at levels similar to those of the wild-type controls. The differences in *AP1* RNA levels among P0, P1 and P2 phenotypic series

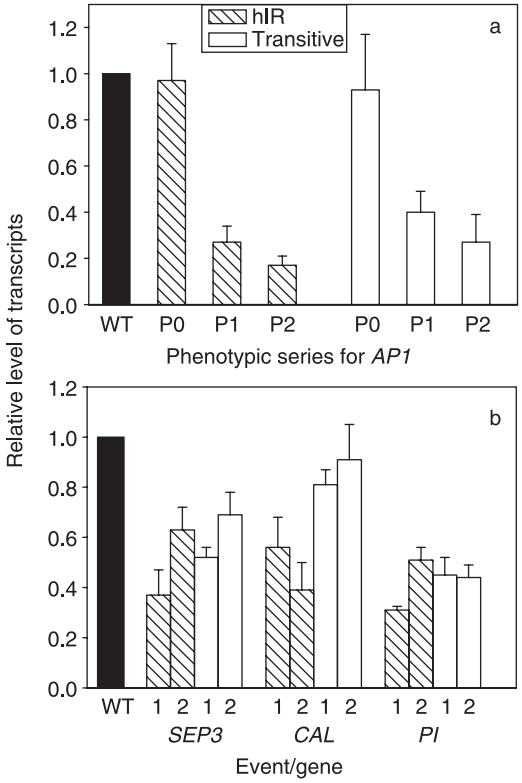

Figure 5 Relative levels of *AP1*, *SEP3*, *CAL* and *PI* transcripts in inflorescences of hIR and transitive *AP1* RNAi knockdown lines. (a) Relative levels of *AP1* transcripts in different phenotypic classes of T_1 transgenics. P0, P1 and P2 indicate phenotypic classes. Each data point represents an average of measurements among three independent events. Measurements were made in triplicate for each individual event. Vertical bars denote standard deviation among three independent events. (b) Relative levels of *SEP3, CAL* and *PI* transcripts in inflorescences of individual pCAPD-AP1 and pCAPT-AP1 knock-down lines showing a strong P2 phenotype. 1 and 2 designate individual events of P2 class. All measurements in (b) for each individual line were made in triplicate. The relative amounts of transcripts were calculated using $2^{-\Delta\Delta Ct}$ method (Livak and Schmittgen, 2001) with data normalized to the expression of *EF1α* as the internal housekeeping gene and using the wild-type control (WT) as an expression reference. hIR and transitive lines are shown by patterned and open bars, respectively. Wild-type controls are shown by filled bars.

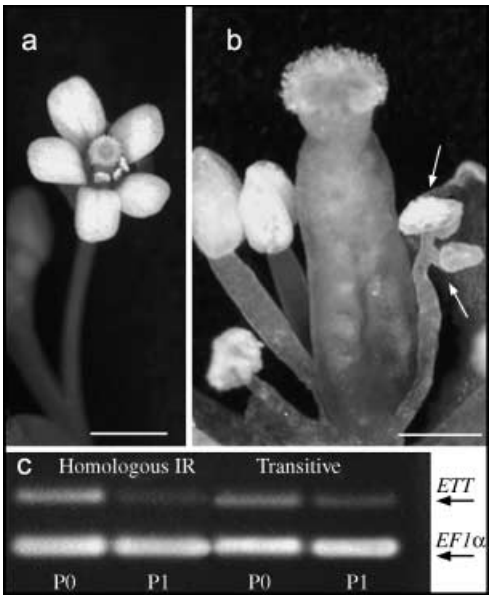

Figure 6 Silencing of *Arabidopsis ETTIN* gene. Phenotypes associated with silencing of *ETTIN* gene using hIR (a) and transitive (b) RNAi constructs. (c) Relative RT-PCR of *ETTIN* transcripts isolated from individual events of different phenotype classes. Each lane shows rRT-PCR products typically representing three independent events.

were further evaluated using Scheffe's method of contrasts. Contrasts estimated using a single degree-of-freedom for P0 vs. P1 and P0 vs. P2 comparisons were significant ($P < 0.01$) for both transitive and hIR lines. However, no significant difference in *AP1* transcripts accumulation was evident among P1 and P2 phenotypic series ($P > 0.05$). The qRT-PCR analysis in inflorescences of individual P2 events (Figure 5b) showed a 40–60% decrease of *PISTILLATA* (*PI*) and *SEPALLATA3* (*SEP3*) transcripts for both types of constructs. The *CAL* transcripts were also down-regulated in hIR but not in transitive pCAPT-AP1 lines, which was consistent with our microarray data.

Efficiency of silencing of the *ETTIN* gene by transitive and hIR constructs

Both transitive and hIR *ETTIN* RNAi transgenics showed expected phenotypic abnormalities such as decreased stamen number or increased perianth organ number (Figure 6). We have not been able to classify *ETTIN* RNAi transgenic lines into continuous phenotypic series (i.e. weak, intermediate and strong) because these abnormalities appeared to occur randomly and separately of each other. Therefore, all observed morphological changes in floral organs of *ETTIN* RNAi lines were assigned to only two phenotypic classes. The P0 plants had no changes in floral organs development as compared to the wild-type controls. The remaining events showing any changes in number of petals or stamens and/or patterning defects in the gynoecium development were classified as P1. The P1 phenotype was observed in approximately 53% and 23% of the T_1 pCAPD-ETT and pCAPT-ETT transformants, respectively (Supplementary Table S1 and Figure 3b). Phenotypic variation among pCAPD-ETT hIR and transitive events was evaluated using Fisher's exact test ($P = 0.04$), indicating that the frequency of occurrence of weaker phenotypic classes among transitive RNAi events was unlikely to be due to chance alone. Analysis of *ETTIN* mRNA using rRT-PCR also confirmed that P1 transgenics of both RNAi types had depleted levels of *ETTIN* mRNA (Figure 6c).

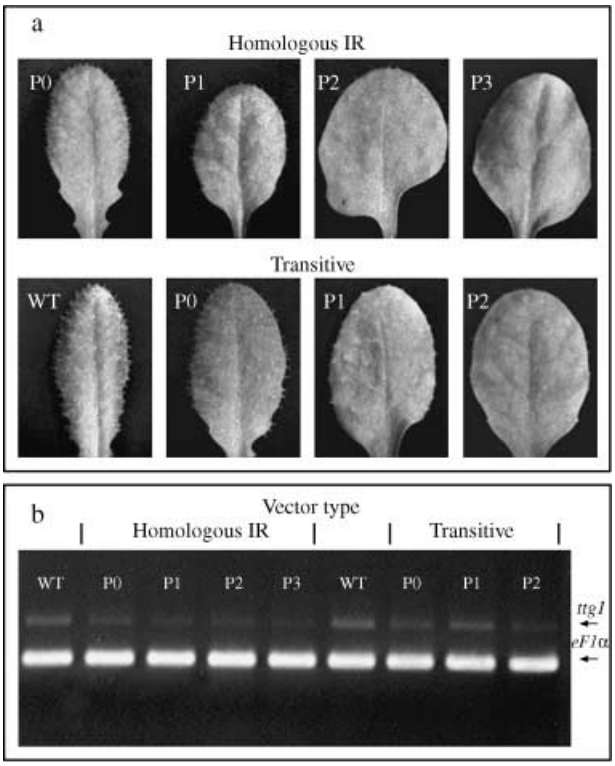

Figure 7 RNAi silencing of *Arabidopsis TTG1* gene using homologous IR and transitive constructs. (a) Phenotypic series observed for hIR (pCAPD-TTG1, top panel) and transitive (pCAPT-TTG1, bottom panel) knock-down lines. P0 corresponds to the weak phenotype undistinguishable from the wild-type control (WT), P3 has trichomless leaves. P1 and P2 comprise phenotypes with intermediate trichome number. Scale bar = 3 mm. Note that P3 phenotype was observed only among pCAPD-TTG1 transgenics. (b) Arrows indicate positions of *TTG1* and *eF1α* RT-PCR fragments. (b) rRT-PCR of *ETTIN* transcripts in pCAPD-TTG1 and pCAPT-TTG1 transgenics. Each lane shows typical amplification representing three individual events of corresponding phenotypic series. Arrows indicate positions of *TTG1* and *eF1α* RT-PCR fragments.

Transitive and hIR silencing of *TTG1* gene

TTG1 RNAi lines were classified into four phenotypic series based on the number of leaf trichomes: P0, P1, P2 and P3 (Figure 7a). The number of trichomes on the rosette's second leaf of P0 plants was similar to that of the wild-type (100–150 per second rosette leaf). The leaves of the P3 lines essentially had no trichomes. Transgenic lines with intermediate numbers of trichomes (70–100 and 30–70 per leaf) were assigned to P1 and P2 phenotypic series, respectively. Results of a semiquantitative rRT-PCR suggested that a reduction in the number of trichomes in P2 and P3 plants was associated with decreased relative levels of *TTG1* mRNA in leaves (Figure 7b). In contrast to hIR pCAPD-TTG1 transgenics, we did not observe the P3 phenotype (trichomeless leaves) among transitive pCAPT-TTG1 lines. However, a shift towards events with a strong phenotype for the *TTG1* hIR construct was not confirmed (Fisher's exact test probability value $P = 0.14$). Low trichome phenotype was stably inherited in homozygous lines of T_3 generation (data not shown).

Discussion

We investigated the relative efficiency of PTGS in *Arabidopsis* caused by transitive and hIR RNAi. To facilitate rapid cloning with the potential of targeting multiple genes, we developed GATEWAY-based vectors suitable for applications in high-throughput plant functional genomics. To evaluate the efficiency of transitive and hIR RNAi we generated a series of vectors containing sequences identical to portions of *AP1*, *ETTIN* and *TTG1* genes. Both types of RNAi constructs induced specific and genetically heritable reduction of function phenotypic changes. However, the hIR constructs, compared with the transitive constructs, generated higher frequencies of loss-of-function phenotypes in all tested genes, although the efficacy of knockdown phenotypes varied by gene (83% with pCAPD-AP1 vs. 53% with pCAPT-ETT). The hIR construct also manifested generally a greater reduction of function phenotypes than the transitive RNAi vector.

We studied *AP1* suppression by hIR and transitive RNAi constructs in detail for two reasons. First, the suppression of *AP1* RNA induced morphological changes which could be classified into a distinct phenotypic series. Second, the *AP1* gene shares extensive sequence homology with several other genes regulating floral development. If either type of *AP1* constructs triggered substantial off-target effects in these genes, they would also cause visible phenotypic changes similar to those described for double *ap1 cal* loss-of-function mutants.

Loss-of-function mutations in floral homeotic gene *AP1* result in a loss or reduction of petals due to the failure to initiate petal primordia leading to the partial conversion of flowers into inflorescence shoots and to disruption of sepal and petal development (Irish and Sussex, 1990; Bowman *et al*., 1993). The transgenics produced by both transitive and homologous IR RNAi *AP1* constructs phenocopied *ap1* reduction or loss-of-function mutants. Both vectors induced changes in floral development similar to those reported for antisense or dsRNA *AP1* interference (Chuang and Meyerowitz, 2000). Phenotypes of hIR and transitive lines were equally enhanced by lower growth temperatures suggesting that this effect (also observed for *ap1* mutants by Bowman *et al*., 1993) is not vector-type specific. Silencing by either hIR or transitive vectors of other target genes used in our study did not show temperature dependency.

The efficient silencing of *AP1* by both hIR and transitive constructs was stably inherited in homozygous lines of T_2 and T_3 generations. The stable inheritance and high penetrance (in excess of 90%) of *AP1* silencing phenotype were consistent with those reported for the similar inverted repeat vectors targeting *AP1* (Chuang and Meyerowitz, 2000) or phytoene desaturase genes (Wang *et al*., 2005).

Both microarray and relative RT-PCR data consistently indicated that the levels of endogenous *AP1* transcripts were depleted in RNAi knockdown lines. The results of a quantitative RT-PCR also indicated that strong (P2) and intermediate (P1) silencing phenotypes were associated with the degradation of *AP1* RNA.

To investigate if genes in the *AP1* regulatory pathway are equally affected by the transitive and hIR RNAi, we evaluated the expression profiles of several other floral genes. *AP1* has been shown to directly and indirectly regulate several floral homeotic genes (Mandel and Yanofsky, 1995; Ferrandiz *et al*., 2000; Ng and Yanofsky, 2001; Lamb *et al*., 2002). For example, *AP1* is required for activation and localized expression of the B-class floral genes *AP3* and *PI* (Ng and Yanofsky, 2001; Lamb *et al*., 2002). Both genes are persistently expressed in petals (Jack *et al*., 1992; Goto and Meyerowitz, 1994), which were reduced or absent in the flowers of RNAi knockdown lines. These two reasons alone offer a possible explanation why *AP1* suppression was associated with the reduced expression of *AP3* and *PI*.

Microarray expression profiling data obtained for *AP1* and three floral homeotic genes, *CAL*, *SEP3* and *PI*, were validated using quantitative RT-PCR. *PI* and *SEP3* were down-regulated in both hIR and transitive lines. Interestingly, qRT-PCR and microarray data consistently indicated that the levels of *CAL* transcripts were decreased in inflorescences of hIR but not transitive transgenics. This result suggests that *AP1* silencing by hIR construct may be potentially associated with moderate off-targeting of the homologous *CAL* transcripts.

Off-targeting effects present a potentially serious problem in RNAi silencing technology both in animals (Jackson *et al*., 2003) and plants (Xu *et al*., 2006). To investigate if off-targeting could be associated with *AP1* silencing induced by transitive or hIR constructs, we studied expression of several genes with sequence homology to *AP1* using microarrays and qRT-PCR.

AP1 shares 76%, 72%, 65%, 61% and 62% of identity at the nucleotide level with *CAL*, *FUL*, *AGL79*, *SEP3* and *SEP2*, respectively. Therefore, these genes could be potential off-targets by the siRNAs generated by degradation of the target *AP1* dsRNA. Computational analysis (using dsCheck off-target search software, Naito *et al*., 2005) predicted that the *CAL* would be the most likely off-target candidate. A full length *AP1* coding sequence could produce 53 and 144 predicted siRNAs with zero or one mismatch to the *CAL* sequence, respectively. The 200-bp *AP1* RNAi fragment we used for both hIR and transitive constructs was designed to have minimal sequence similarity to *CAL* and other homologous genes. Nevertheless, a fragment-limited search still predicted 5 and 17 siRNAs with 1 and 2 nucleotide mismatches, respectively, which could potentially trigger off-target *CAL* silencing. Both microarray and qRT-PCR data suggested that the *CAL* gene was down-regulated in hIR but not in transitive lines and that a moderate off-targeting effect could be triggered by the *AP1* hIR construct. However, a decline in *CAL* transcript levels in hIR transgenics apparently was not sufficient to phenocopy the *ap1 cal* double mutant (Bowman *et al*., 1993). Altogether, our data suggested that the targeting of the least conserved portion of the *AP1* gene by both hIR and transitive constructs was specific. Off-target RNAi effects were minimal in spite of the prediction of a few siRNAs potentially capable to trigger transitive silencing of *CAL* gene.

Similar to loss-of-function *ett* mutants (Sessions and Zambryski, 1995) the suppression of *ETTIN* by both hIR and transitive vectors resulted in reduced or increased number of floral organs such as petals and stamens and in more rare instances – in abnormal development of the gynoecium. Consistently with *AP1*, hIR construct targeting *ETTIN* generated significantly more transgenics with visible phenotypic changes than the transitive construct.

Loss-of-function *ttg1* mutants demonstrate impaired development of root hairs and leaf trichomes (Walker *et al*., 1999). In our experiments, both hIR and transitive RNAi knockdown lines showing reduced trichome number phenotype also have had depleted levels of *TTG1* mRNA. We did not, however, find a statistically significant shift towards events with a strong phenotype for the *TTG1* hIR construct. However, near complete trichome development suppression was observed only among hIR but not among transitive RNAi transgenics. This suggests that *TTG1* silencing was also more efficient by using inverted repeat vector.

Our hIR and transitive GATEWAY-based vectors offer different sets of advantages for generating and screening RNAi transgenics. In our hands, the majority of hIR constructs yielded higher frequencies of transgenic events with strong RNAi suppression phenotypes compared to transitive constructs. However, the transitive vectors could be a method of choice when (i) high throughput generation of stable constructs carrying single or multiple inserts of unrelated genes is required (e.g. cDNA libraries screening), and (ii) complete

silencing of the target gene is expected to be lethal for the plant development. Transitive vectors also allow monitoring the efficiency of transitive RNAi spreading along single or multiple gene fragments via silencing of a linked reporter gene in the transgenic host, although the efficacy of this approach remains to be studied. Each type of vector has a distinct set of advantages and their combination provides effective tools for applications in plant functional genomics and biotechnology.

Experimental procedures

Plant genotypes, growth conditions, bacterial strains and vectors

Arabidopsis loss-of-function mutants *ap1* (stocks #CS28, CS6231, CS6232), *ett* (stocks #CS8554, CS8555) and *ttg1* (stock #CS277) were obtained from *Arabidopsis* Biological Resource Center (ABRC). Ecotype Columbia 0 of *Arabidopsis* was used for all transformations. All lines were grown under the same conditions as the transgenics and used for comparative phenotyping. For phenotype scoring *AP1* knockdown transgenics were grown at 15 °C. To obtain seeds from P2 *AP1* RNAi knockdown lines plants were grown at 21 °C.

Agrobacterium tumefaciens strain C58/pMP90 (GV3101), a disarmed derivative of the nopaline C58 strain, was transformed by the freeze-thaw method (Holstein *et al*., 1978). *Escherichia coli* strain Top 10 (Invitrogen) was used in all cloning procedures. *Arabidopsis* transformation was performed by a floral dip method (Clough and Bent, 1998) modified as described previously (Filichkin *et al*., 2004). To obtain primary T_1 transformants T_0 seeds (a mixture of transgenic and non-transgenic seeds from the wild-type plants) were germinated on MS medium supplied with 25 μg/mL of kanamycin. The statistical distribution of phenotypic classes among kanamycin-resistant T_1 transformants was analysed by χ^2-test for independence or Fisher's exact test using Statistix 8.0 software (Analytical Software, Tallahassee, FL, USA).

Homozygous pCAP-AP1 lines showing P2 phenotype were isolated by consequent rounds of selection. The seeds from individual independent pCAP-AP1 events of T_1 generation showing P2 phenotype were plated on kanamycin-containing plates. The ratio of kanamycin-resistant to kanamycin-sensitive seedlings was calculated and statistically analysed using χ^2 goodness-of-fit test. T_2 progeny of kanamycin-resistant plants showing simple Mendelian inheritance pattern (3 : 1) was subjected to a second round of selection. T_3 lines showing near 100% kanamycin-resistant pattern were further propagated in soil and scored for the inheritance of RNAi suppression phenotype.

RNA isolation, analysis, relative and quantitative RT-PCR

Total cellular RNA from plant tissues was isolated using Plant RNA Reagent (Invitrogen). Isolated RNA was treated with RNase-free DNase (Ambion, Austin, TX, USA) and additionally purified using Qiagen RNA isolation kit (Qiagen, Valencia, CA, USA) according to the manufacturer's protocols. RNA concentration, integrity and 28S/18S rRNA ratio were estimated using Agilent 2100 Bioanalyser (Agilent Technologies, Palo Alto, CA, USA). The first strand of cDNA was synthesized using 1 μg of total RNA, poly(A) oligonucleotide and Superscript™ III First strand cDNA synthesis kit (Invitrogen) according to the manufacturer's protocol.

Relative RT-PCR (rRT-PCR) was performed using two sets of primers: one pair for the amplification of cDNA from a reference gene *EF1α* and another corresponding to cDNA of a target gene. The primers were designed not to overlap the fragments of sequences introduced into RNAi constructs. To avoid the amplification of genomic DNA *AP1* and *ETTIN* primers were designed to encompass the introns of the respective genes. The sequences of primers and the sizes of expected RT-PCR products are compiled in Supplementary Table S2. The distribution of levels of *AP1* transcripts among phenotypic series was analysed by ANOVA using Scheffe's F method of contrasts and Statistix 8.0 software (Analytical Software).

Genomic DNA isolation and PCR amplification

To confirm transgene presence, genomic DNA was isolated from *Arabidopsis* leaves using the Plant DNAeasy Kit (Qiagen) according to the manufacturer's instructions. Approximately 25–50 ng of DNA was used as a template for PCR. The transgene presence was confirmed by PCR using *nptII*-specific primers (5′-ATCCATCATGGCTGATGCAATGCG-3′ and 5′-CCATGATATTCGGCAAGCAGGCAT-3′) to amplify 253 bp of T-DNA insertion. To amplify the *NPTII* gene fragment, the reactions were subjected to 30 cycles of PCR (94 °C for 1 min, 58 °C for 1 min and 72 °C for 1 min). The PCR products were separated on 1% agarose gels and stained with ethidium bromide.

Vector construction

Binary vectors for homologous IR and transitive RNAi were constructed using pART27 backbone (Gleave, 1992). We used the GATEWAY™ Conversion System (reading frame A) (Invitrogen) to incorporate the proper recombination sites and genes for negative and positive selection. The conversion cassette contains *attR* recombination sites flanking a *ccdB* gene and a chloramphenicol resistance gene for negative and positive selection of recombinants in *E. coli*. The pCAPD vector contains two cassettes in inverse orientation, flanking the *PIV2* intron from potato (Vancanneyt *et al*., 1990). Transcription is terminated by the *Agrobacterium OCS* terminator. The pCAPT vector contains a single conversion cassette upstream of an inverted repeat of the octopine synthase (*OCS*) terminator. In addition, pCAPT contains a small fragment of the modified green fluorescent protein gene (*GFP*) (Haseloff *et al*., 1997) upstream of the GATEWAY recombination site to monitor the efficiency of transitive silencing in transgenic plants over-expressing GFP protein. In both pCAPD and pCAPT, the expression of hairpin RNA cassettes is under the control of an identical portion of a constitutive CaMV 35S promoter. Both vectors contain spectinomycin and kanamycin (*NPTII*) resistance genes for the selection in bacteria and plants, respectively.

Approximately 200 bp target fragments of three *Arabidopsis* target genes (gene descriptions and primer sequences are available online in Supplementary Table S2) were PCR amplified using primers with tails corresponding to *attB* recombination sites. GATEWAY entry clones were created using BP Clonase™ enzyme-mediated recombination (Invitrogen). Target gene fragments were further cloned into the PCAPD and pCAPT binary vectors using LR Clonase™

II enzyme mix (Invitrogen) according to the manufacturer's protocol. All final constructs were verified by sequencing.

Microarray analysis

Total RNA was isolated from the inflorescences of *Arabidopsis* RNAi transgenics of the T_1 generation as well as the wild-type control plants. The quantity and quality of isolated RNA were evaluated using NanoDrop spectrophotometer (NanoDrop Technologies, Wilmington, DE, USA) and Bioanalyser (Agilent Technologies). cDNA and biotinylated cRNA were prepared from 1 μg RNA using the MessageAmp™ II-Biotin Enhanced Kit (Ambion). Target amplification, labelling and fragmentation were carried out according to the manufacturer's instructions. The size of resulting biotinylated cRNA fragments was in a range of 50–200 bp. We used *Arabidopsis* genome-wide spotted 70-mer oligo microarrays containing approximately 29 000 elements (a detailed microarray description is available at http://ag.arizona.edu/microarray; complete array element sequence information is available at http://omad.operon.com/download/index.php). A total of 10 microarrays were used for the hybridizations. The experiment was duplicated, using two biological samples (two independent transgenic pCAPT-AP1 and pCAPD-AP1 lines) and each biological replicate was treated in two technical replicates (individual hybridizations).

Pre-hybridization was carried out in a hybridization chamber (Corning, Acton, MA, USA) using 0.1 μg/μL herring sperm DNA, 0.5 μg/μL acetylated bovine serum albumin (BSA) and 1× 2-morpholinoethanesulphonic acid (MES) hybridization buffer at 42 °C for 15 min. Arrays were prepared for hybridization by briefly washing the prehybridized slides in water and absolute ethanol followed by spin-drying. Hybridizations were carried out using 10.0 μg of fragmented biotinylated cRNA in a solution containing 0.1 μg/μL herring sperm DNA, 0.5 μg/μL BSA and 1× MES hybridization buffer at 42 °C for 16 h. Post-hybridization washes included two 1-min washes with 6× SSPE buffer (Sambrook *et al*., 1989) and 0.01% Tween-20 solution at room temperature, two 15-min washes with 1× MES buffer, 0.026 M NaCl and 0.01% Tween-20 at 45 °C followed by a 1-min wash with 6× SSPE buffer supplied with 0.01% Tween-20. Staining was carried out at room temperature in solution containing 100 mM sodium solution (pH 6.5), 1 M sodium chloride, 0.05% Tween-20, 2 μg/μL BSA and 0.01 μg/μL streptavidin-Alexa Fluor® 555 conjugate (Invitrogen) for 15 min. Following a final wash with 3× SSPE and 0.005% Tween-20, the slides were spin-dried and scanned using ScanArray Express 5000 (PerkinElmer, Wellesley, MA, USA) with laser and photo multiplier tube settings of 90 and 65, respectively. For compensation of differences in probe labelling and non-linearity of signal intensities microarray data were normalized using locally weighted polynomial regression (LOWESS) method and Imagene 6.1 software (BioDiscovery, El Segundo, CA, USA).

Acknowledgements

This work was supported in part by grants from the US Department of Energy (award number 4000023558 'Genome-enabled discovery of carbon sequestration genes in poplar'), the National Science Foundation Industry/University Co-operative Research Centers (award number 9980423) and by industrial members of the Tree Biosafety and Genomics Research Cooperative at Oregon State University (http://wwwdata.forestry.oregonstate.edu/tgb).

References

Baulcombe, D. (2004) RNA silencing in plants. *Nature*, **431**, 356–363.

Bleys, A., Vermeersch, L., Van Houdt, H. and Depicker, A. (2006) The frequency and efficiency of endogene suppression by transitive silencing signals is influenced by the length of sequence homology. *Plant Physiol*. **142**, 788–796.

Bowman, J.L., Alvarez, J., Weigel, D., Meyerowitz, E.M. and Smyth, D.R. (1993) Control of flower development in *Arabidopsis thaliana* by *APETALA1* and interacting genes. *Development*, **119**, 721–743.

Braunstein, T.H., Moury, B., Johannessen, M. and Albrechtsen, M. (2002) Specific degradation of 3′ regions of GUS mRNA in post-transcriptionally silenced tobacco lines may be related to 5′–3′ spreading of silencing. *RNA*, **8**, 1034–1044.

Brummell, D.A., Balint-Kurti, P.J., Harpster, M.H., Palys, J.M., Oeller, P.W. and Gutterson, N. (2003) Inverted repeat of a heterologous 3′-untranslated region for high-efficiency, high-throughput gene silencing. *Plant J*. **33**, 793–800.

Carrington, J.C. and Ambros, V. (2003) Role of microRNAs in plant and animal development. *Science*, **301**, 336–338.

Chen, S., Hofius, D., Sonnewald, U. and Bornke, F. (2003) Temporal and spatial control of gene silencing in transgenic plants by inducible expression of double-stranded RNA. *Plant J*. **36**, 731–740.

Chuang, C.-F. and Meyerowitz, E.M. (2000) Specific and heritable genetic interference by double-stranded RNA in *Arabidopsis thaliana*. *Proc. Natl. Acad. Sci. USA*, **97**, 4985–4990.

Clough, S.J. and Bent, A.F. (1998) Floral dip: a simplified method for *Agrobacterium*-mediated transformation of *Arabidopsis thaliana*. *Plant J*. **16**, 735–743.

Ferrandiz, C., Gu, Q., Martienssen, R. and Yanofsky, M.F. (2000) Redundant regulation of meristem identity and plant architecture by *FRUITFULL, APETALA1* and *CAULIFLOWER*. *Development*, **127**, 725–734.

Filichkin, S.A., Leonard, J.M., Monteros, A., Liu, P.P. and Nonogaki, H. (2004) A novel endo-β-mannanase gene *LeMAN5* in tomato is associated with anther and pollen development. *Plant Physiol*. **134**, 1080–1087.

Gleave, A.P. (1992) A versatile binary vector system with a T-DNA organisational structure conducive to efficient integration of cloned DNA into the plant genome. *Plant Mol. Biol*. **20**, 1203–1207.

Goto, K. and Meyerowitz, E.M. (1994) Function and regulation of the *Arabidopsis* floral homeotic gene *PISTILLATA*. *Genes Dev*. **8**, 1548–1560.

Hamilton, A.J., Brown, S., Yuanhai, H., Ishizuka, M., Lowe, A., Alpuche Solis, A.-G. and Grierson, D. (1998) A transgene with repeated DNA causes high frequency, post-transcriptional suppression of *ACC*-oxidase gene expression in tomato. *Plant J*. **15**, 737–746.

Haseloff, J., Siemering, K.R., Prasher, D.C. and Hodge, S. (1997) Removal of a cryptic intron and subcellular localization of green fluorescent protein are required to mark transgenic *Arabidopsis* plants brightly. *Proc. Natl. Acad. Sci. USA*, **94**, 2122–2127.

Helliwell, C.A. and Waterhouse, P.M. (2005) Constructs and methods for hairpin RNA-mediated gene silencing in plants. *Methods Enzymol*. **392**, 24–35.

Holstein, M., De Wacek, D., Depicker, A., Messers, E., van Montagu, M. and Schell, J. (1978) Transfection and transformation of *Agrobacterium tumefaciens*. *Mol. Gen. Genet*. **163**, 181–187.

Irish, V.F. and Sussex, I.M. (1990) Function of the apetala-1 gene during Arabidopsis floral development. *Plant Cell*, **2**, 741–753.

Jack, T., Brockman, L.L. and Meyerowitz, E.M. (1992) The homeotic gene *APETALA3* of *Arabidopsis thaliana* encodes a MADS box and is expressed in petals and stamens. *Cell*, **68**, 683–697.

Jackson, A.L., Bartz, S.R., Schelter, J., Kobayashi, S.V., Burchard, J., Mao, M., Li, B., Cavet, G. and Linsley, P.S. (2003) Expression profiling reveals off-target gene regulation by RNAi. *Nat. Biotechnol*. **21**, 635–637.

Lamb, R.S., Hill, T.A., Tan, Q.K.-G. and Irish, V.F. (2002) Regulation of *APETALA3* floral homeotic gene expression by meristem identity genes. *Development*, **129**, 2079–2086.

Lipardi, C., Wei, Q. and Paterson, B.M. (2001) RNAi as random degradative PCR: siRNA primers convert mRNA into dsRNAs that are degraded to generate new siRNAs. *Cell*, **107**, 297–307.

Livak, K.J. and Schmittgen, T.D. (2001) Analysis of relative gene expression data using real-time quantitative PCR and the $2^{-\Delta\Delta Ct}$ method. *Methods*, **25**, 402–408.

Lo, C., Wang, N. and Lam, E. (2005) Inducible double-stranded RNA expression activates reversible transcript turnover and stable translational suppression of a target gene in transgenic tobacco. *FEBS Lett*. **579**, 1498–1502.

Mandel, M.A., Gustafson-Brown, C., Savidge, B. and Yanofsky, M.F. (1992) Molecular characterization of the *Arabidopsis* floral homeotic gene *APETALA1*. *Nature*, **360**, 273–277.

Mandel, M.A. and Yanofsky, M.F. (1995) The *Arabidopsis* AGL8 MADS box gene is expressed in inflorescence meristems and is negatively regulated by *APETALA1*. *Plant Cell*, **7**, 1763–1771.

Meister, G. and Tuschl, T. (2004) Mechanisms of gene silencing by double-stranded RNA. *Nature*, **431**, 343–349.

Naito, Y., Yamada, T., Matsumiya, T., Ui-Tei, K., Saigo, K. and Morishita, S. (2005) dsCheck: highly sensitive off-target search software for double-stranded RNA-mediated RNA interference. *Nucleic Acids Res*. **33**, W589–W591.

Ng, M. and Yanofsky, M.F. (2001) Activation of the *Arabidopsis* B class homeotic genes by APETALA1. *Plant Cell*, **13**, 739–753.

Nicolas, F.E., Torres-Martinez, S. and Ruiz-Vazquez, R.M. (2003) Two classes of small antisense RNAs in fungal RNA silencing triggered by nonintegrative transgenes. *EMBO J*. **22**, 3983–3991.

Sambrook, J., Fritsch, E.F. and Maniatis, T. (1989) *Molecular Cloning: A Laboratory Manual*, 2nd edn. Cold Spring Harbor, NY: Cold Spring Harbor Laboratory Press.

Sessions, A. and Zambryski, P.C. (1995) *Arabidopsis* gynoecium structure in the wild type and in *ettin* mutants. *Development*, **121**, 1519–1532.

Sijen, T., Fleenor, J., Simmer, F., Thijssen, K.L., Parrish, S., Timmons, L., Plasterk, R.H. and Fire, A. (2001) On the role of RNA amplification in dsRNA-triggered gene silencing. *Cell*, **107**, 465–476.

Smith, N.A., Singh, S.P., Wang, M.-B., Stoutjesdijk, P., Green, A. and Waterhouse, P.M. (2000) Total silencing by intron-spliced hairpin RNAs. *Nature*, **407**, 319–320.

Tang, G., Reinhart, B.J., Bartel, D.P. and Zamore, P.D. (2003) A biochemical framework for RNA silencing in plants. *Genes Dev*. **17**, 49–63.

Tomari, Y. and Zamore, P.D. (2005) Perspective: machines for RNAi. *Genes Dev*. **19**, 517–529.

Vaistij, F.E., Jones, L. and Baulcombe, D.C. (2002) Spreading of RNA targeting and DNA methylation in RNA silencing requires transcription of the target gene and a putative RNA-dependent RNA polymerase. *Plant Cell*, **14**, 857–867.

Van Houdt, H., Bleys, A. and Depicker, A. (2003) RNA target sequences promote spreading of RNA silencing. *Plant Physiol*. **131**, 245–253.

Vancanneyt, G., Schmidt, R., O'Connor-Sanchez, A., Willmitzer, L. and Rocha-Sosa, M. (1990) Construction of an intron-containing marker gene: splicing of the intron in transgenic plants and its use in monitoring early events in *Agrobacterium*-mediated plant transformation. *Mol. Gen. Genet*. **220**, 245–250.

Vazquez, F., Vaucheret, H., Rajagopalan, R., Lepers, C., Gasciolli, V., Mallory, A.C., Hilbert, J.L., Bartel, D.P. and Crete, P. (2004) Endogenous trans-acting siRNAs regulate the accumulation of *Arabidopsis* mRNAs. *Mol. Cell*, **16**, 69–79.

Voinnet, O., Vain, P., Angell, S. and Baulcombe, D.C. (1998) Systemic spread of sequence-specific transgene RNA degradation in plants is initiated by localized introduction of ectopic promoterless DNA. *Cell*, **95**, 177–187.

Walker, A.R., Davison, P.A., Bolognesi-Winfield, A.C., James, C.M., Srinivasan, N., Blundell, T.L., Esch, J.J., Marks, M.D. and Gray, J.C. (1999) The *TRANSPARENT TESTA GLABRA1* locus, which regulates trichome differentiation and anthocyanin biosynthesis in *Arabidopsis*, encodes a WD40 repeat protein. *Plant Cell*, **11**, 1337–1350.

Wang, T., Iyer, L.M., Pancholy, R., Shi, X. and Hall, T.C. (2005) Assessment of penetrance and expressivity of RNAi-mediated silencing of the *Arabidopsis* phytoene desaturase gene. *New Phytol*. **167**, 751–760.

Waterhouse, P.M., Graham, M.W. and Wang, M.B. (1998) Virus resistance and gene silencing in plants can be induced by simultaneous expression of sense and antisense RNA. *Proc. Natl. Acad. Sci. USA*, **95**, 13959–13964.

Wesley, S.V., Helliwell, C.A., Smith, N.A., Wang, M., Rouse, D.T., Liu, Q., Gooding, P.S., Singh, S.P., Abbott, D., Stoutjesdijk, P.A., Robinson, S.P., Gleave, A.P., Green, A.G. and Waterhouse, P.M. (2001) Construct design for efficient, effective and high-throughput gene silencing in plants. *Plant J*. **27**, 581–590.

Xu, P., Zhang, Y., Kang, L., Roossinck, M.J. and Mysore, K.S. (2006) Computational estimation and experimental verification of off-target silencing during posttranscriptional gene silencing in plants. *Plant Physiol*. **142**, 429–440.

Supplementary material

The following supplementary material is available for this article:

Figure S1 Hierarchical analysis of gene expression in inflorescences of hIR and transitive RNAi transgenics. (A) Hierarchical clustering of all individual replicates. (B) Close up of (A). (C) Clustering of samples according to the RNAi type. Red and green represent elevated and reduced expression relative to the normalized average signal intensity, respectively. hIR and transitive RNAi samples form a common branch on hierarchical tree. WT – wild type, IR1, IR2 and TR1, TR2 designate individual hIR and transitive RNAi lines, respectively. 1 and 2 indicate individual technical replicates of each biological sample (transgenic line).

Figure S2 Expression profiles of *AP1* and several selected floral developmental genes in inflorescences of pCAPD-AP1 and pCAPT-AP1 knock-down lines. Microarrays were hybridized with the total RNA isolated from the inflorescences and analyzed as described in Experimental Procedures. Each point represents an average of normalized intensities of two biological replicates (two independent transgenic lines) including two hybridization replicates for each line. Vertical bars denote standard deviation. "v" symbol denotes down-regulated genes; "^" shows up-regulated genes and "*" indicates no changes in gene expression at confidence level $P<0.05$. Vertical line l demarcates symbols of gene expression in hIR (left), or in transitive (right) lines. The graph was generated using GeneSpring GX 7.2 software. At1g07940, elongation factor *EF1α* (used as an example of ubiquitously expressed internal control gene). Gene identifications: At3g02310, developmental gene *SEPALLATA2* (*SEP2*) identical to GB:P29384; At3g54340, floral homeotic gene *APETALA3* (*AP3*). At5g20240, floral homeotic gene *PISTILLATA* (*PI*); At1g24260, MADS-box gene *SEPALLATA3* (*SEP3*) strongly similar to GB:O22456; At1g69120, floral homeotic gene *APETALA1* (*AP1*) identical to SPlP35631; At5g61850, floral meristem identity control gene *LEAFY* (*LFY*); At5g60910, floral agamous-like MADS box homeotic gene *FRUITFULL* (*AGL8*); At1g26310, floral homeotic MADS-box gene *CAULIFLOWER* (*CAL*) sharing strong sequence homology with *AP1*; At3g30260, MADS-box gene (*AGL79*).

Table S1 (A) Number of independent primary transformants in phenotypic series generated by the transitive and hIR vectors. (B) Inheritance of *AP1* silencing phenotype among hIR and transitive transgenic lines

Table S2 Target genes and primers used for PCR amplification, construct assembly, confirmation of transgenics, rRT-PCR and qRT-PCR

Table S3 List of genes differentially expressed in both pCAPD-AP1 and.pCAPT-AP1 transgenics

This material is available as part of the online article from: http://www.blackwell-synergy.com/doi/abs/10.1111/j.1467-7652.2007.00267.x
(This link will take you to the article abstract).

Please note: Blackwell Publishing are not responsible for the content or functionality of any supplementary materials supplied by the authors. Any queries (other than missing material) should be directed to the corresponding author for the article.

